ORIGINAL CONTRIBUTION

Sedimentation and drying dissipative patterns of colloidal silica (560 nm in diameter) suspensions in a glass dish and a watch glass

Tsuneo Okubo

Abstract The sedimentation and drying dissipative structural patterns formed during the course of drying colloidal silica spheres (CS550, 560 nm in diameter) in an aqueous suspension have been studied in a glass dish and a watch glass. Broad ring patterns were formed within 20 min in the suspension state by the convectional flow of the colloidal spheres and water. The sedimentary spheres always moved by the convectional flow of water, and the broad ring patterns became sharp with time. The sharpness of the broad rings was sensitive to the change in the room temperature and/or humidity. Colorful macroscopic structures were composed of the broad ring and wave-like patterns, and further colorful and beautiful microscopic fine patterns formed during the solidification processes based on the convectional and sedimentation structures. The drying patterns of the colloidal suspensions containing sodium chloride were different from the structures of CS550 or sodium chloride individuals, which support the synchronous cooperative interactions between the colloidal spheres and the salts.

Keywords Sedimentation dissipative structure ·
Drying dissipative structure · Pattern formation ·
Colloidal silica spheres · Broad ring pattern ·
Wave-like pattern

T. Okubo (✉)
Institute for Colloidal Organization,
Hatoyama 3-1-112, Uji,
Kyoto 611-0012, Japan
e-mail: okubotsu@ybb.ne.jp

Introduction

Most structural patterns in nature are formed via self-organization accompanied by the dissipation of free energy and in the nonequilibrium state. Among the several factors in the free energy dissipation of aqueous colloidal suspensions, evaporation of the solvent molecules at the air-solvent interface and gravitational convection are very important. To understand the mechanisms of the dissipative self-organization of simple model systems instead of the more complex nature itself, the authors have systematically studied the *convectional*, *sedimentation*, and *drying* dissipative patterns of suspensions and solutions.

Several papers on the drying pattern formation of colloidal suspensions have already been reported [1–16]. Electrostatic interparticle interactions have been pointed out as one of the important factors for the dissipative structures. Hydrophobic and hydrophilic interactions were also demonstrated to be important during the drying processes [13–16]. Gelbart et al. [5, 7] examined the mechanism of solvent evaporation in broad rings formed by drying metal colloids on a substrate. Haw [17], Narita et al. [18], and Mahesh et al. [19] studied the dynamic and phase transitional processes during drying. Shimomura et al. [20] and other researchers have intensively studied the dissipative patterns when drying polymer solutions.

Recently, the drying, sedimentation, and convectional dissipative patterns have been reported by the authors for suspensions and solutions, colloidal silica spheres, polystyrene spheres, plate-like fractionated bentonite particles, green tea, Chinese black ink, simple electrolytes, linear-type polyelectrolytes, water-soluble nonionic polymers, biopolymers, gels, and detergents [21–41]. The variety of the dissipative patterns that has been observed is compiled in Table 1, in which the patterns observed in this study are also listed.

Table 1 Patterns observed during the course of drying the suspensions and solutions

Drying patterns				
Macroscopic	Broad ring	Normal BR	Single BR	[21–28, 30–36, 38–41, this work]
			Multiple BR	[23, 28, 30, 34, 35, 38]
			Square broad band	[37]
		Notched BR		[21, 22, 41]
		Inner and outer BR		[38, 40]
		Multiple fine circles		[25]
	Spoke-like lines	SL crack		[21, 22, 26, 36, 38]
		SL hill	Normal SLH	[25]
			Flickering SLH	[35]
	Ring-like pattern	RL crack		[21, 22, 30]
	Wave-like pattern			[26, 30, 39, this work]
	Column-like pattern			[37]
	Central round hill			[27, 29, 30, 35]
Microscopic	Fine multiple SL line	FMSL crack		[21, 22, 33, 35, 36, 39, 40, this work]
	FM ring line	FM ring crack		[33, 35, 39, this work]
	Branch-like			[21, 24, 26–29]
	Earth worm-like			[22]
	String-like			[23, 28, 29, 32]
	Dendrite-like, leaf-like			[31, 39, this work]
	Star-like			[23, 27–29, 31, 39, this work]
	Street road-like			[23, 38, 41]
	Flower-like			[23, 24, 35, 38, 41]
	Block-like	Normal block-like		[27–29, 34, 35, 38]
		"Shigaraki Yaki"-like		[25]
	Cross-like			[24, 30, 38]
	Rod-like			[38]
	Arc-like			[24]
	Needle-like			[41]
	Wrinkled pattern			[27, 30]
	Chapped pattern			[27, 30]
	Netting pattern			[26]
Sedimentation pattern				
Macroscopic	Broad ring			[31–34, 39, this work]
Microscopic	Vague wrinkled pattern			[27]
Convectional pattern				
Macroscopic	Spoke-like lines			[25, 42–44]
	Hexagonal circulating cells ("Bernard" cell)			[45]
	Cyclic circulating cells			[25]
	Smoke-like			[25]
	Cooperative circulation			[33]
Microscopic	Cell convections ("Terada" cell)			[25, 42–44]

Macroscopic broad ring patterns of the hill accumulated with spheres in the outside edges are always formed. For the nonspherical particles, a central round hill was formed in the central area in addition to the broad ring. Macroscopic spoke-like cracks or fine hills including flickering spoke-like ones were also observed for many solutes. The convection of water and the solute molecules at different rates under gravity and the translational and rotational Brownian movement of the latter were important for the macroscopic pattern formation. Furthermore, so many types of beautiful fractal patterns such as branch-like, arc-like, block-like, star-like, cross-like, and string-like ones were observed in the microscopic scale. These microscopic drying patterns were reflected from the *shape*, *size*, and *flexibility* of the solute molecules themselves. Microscopic patterns also supported importance of the electrostatic and the hydrophobic interactions between solutes and/or between the solutes and substrate in the course of solidification. One of the important findings in our experiments was that the primitive vague patterns formed already in the suspension state before dryness and they grew toward fine structures in the course of solidification.

The broad ring patterns were also formed within 30 min in suspension state at room temperature by the convectional flow of water and the colloidal particles. The important finding here was that the sedimentary particles were suspended above the substrate and always moved by the external fields including convectional flow and the sedimentation of the particles by gravity. It should be noted that the existence of the small circle-like *cell convections* ("Saibo-uzu" in Japanese), proposed by Terada et al. [42–44], for the first time, was supported. A vigorous convectional cell-like flow was visually observed for the suspensions, and the patterns dynamically changed with time. It should be mentioned that the distinction of the micro- and macrostructures is arbitrary because the dissipative patterns are stratified on both micro- to macroscales. However, the authors often state that the patterns in the order of larger than and smaller than 1 mm as macro- and microstructures, respectively. Furthermore, hexagonal circulating cells ("Bernard" cell) are also well known as one of the macroscopic convectional dissipative patterns [45].

In this study, the sedimentation and drying dissipative patterns of colloidal silica spheres, 560 nm in diameter, were studied in a glass dish and a watch glass on macroscopic and microscopic scales. One of the main purposes of this study is to investigate the sphere size dependence of the dissipative structures.

Experimental

Materials

CS550 silica spheres were donated by the Catalysts & Chemicals Ind. (Tokyo). The diameter, standard deviation of the mean diameter, and polydispersity index of the spheres were 560, 17.6, and 0.031 nm, respectively. These size parameters were determined using an electron microscope at Gifu University (Hitachi H8100). The spheres were carefully purified by repeated decantation of more than 30 times. The sample was then treated on a mixed bed of cation- and anion-exchange resins [Bio-Rad, AG501-X8 (D), 20–50 mesh] for 6 years before use because newly produced silica spheres always release a considerable amount of alkali ions from the porous sphere surfaces for a long time. The water used for the sample preparation was purified by a Milli-Q reagent grade system (Milli-RO5 plus and Milli-Q plus, Millipore, Bedford, MA, USA).

Observation of the dissipative structures

A 10- or 4-ml aliquot of the aqueous suspension of CS550 sample was carefully and gently placed into a glass dish (42 mm inner diameter and 15 mm height, code 305-02, TOP, Tokyo) or a medium size watch glass (70 mm diameter, TOP, Tokyo), respectively. Observations of the sedimentation and drying patterns were made for the suspensions set on a desk until completely dried in an air-conditioned room at 27 °C. The humidity of the room air in the laboratory was between 64 and 69%, which was not regulated. The concentrations of CS550 and NaCl ranged from 0.000827 to 0.00827 in volume fraction and from 0.0001 to 0.03 M, respectively.

Macroscopic dissipative structures were observed using a Canon EOS 10D digital camera (Canon, Tokyo) with a EF 28–200 mm lens (f=3.5–5.6 USM, Canon). The microscopic structures were observed using a metallurgical microscope (PME-3, Olympus, Tokyo).

Results and discussion

Sedimentation and drying dissipative patterns in a glass dish

Figure 1 shows the sedimentation (subpanels a to d) and drying patterns (subpanels e and f) of CS550 spheres when the sphere concentration is very low, 0.000827 in volume fraction. Broad ring patterns were clearly observed within several tens of minutes (ca. 20 min) for the suspensions without a cap, and the suspensions dried up after 6.9 days. It should be recalled that the broad ring patterns also did not appear at all in a dish with a cap for the colloidal silica spheres, 1.2 μm and 300 nm in diameter [31, 39]. In the suspension state with a cap, they also exhibited the broad ring patterns after a very long time, and the dried film showed very strong iridescent colors. Furthermore, very fine and beautiful fractal structures were observed for the dried film using a microscope. This shows that the shielding of a glass dish with a cap is not very complete for preventing the evaporation. However, the evaporation and the resulting convectional flow are, of course, efficiently retarded with a cap. It should be noted that the broad rings formed rather quickly within several tens of minutes after the suspension was set and during the stage of the incomplete sedimentation of the spheres, which shows that the convectional flow of water and spheres are vigorous even at room temperature.

The main cause for the broad ring formation is due to the convection flow of water and CS550 spheres at the different rates, where the rate of the latter will be slower than that of the former under gravity. Especially, the flow of the spheres from the center area toward the outside edges in the lower layers of the liquid, which was observed by a digital HD microscope directly from the movement of the very rarely occurred aggregates of Chinese black ink, is important [25]. Clearly, the convectional flow is enhanced by the evaporation of water at the liquid surface, resulting in a lowering of
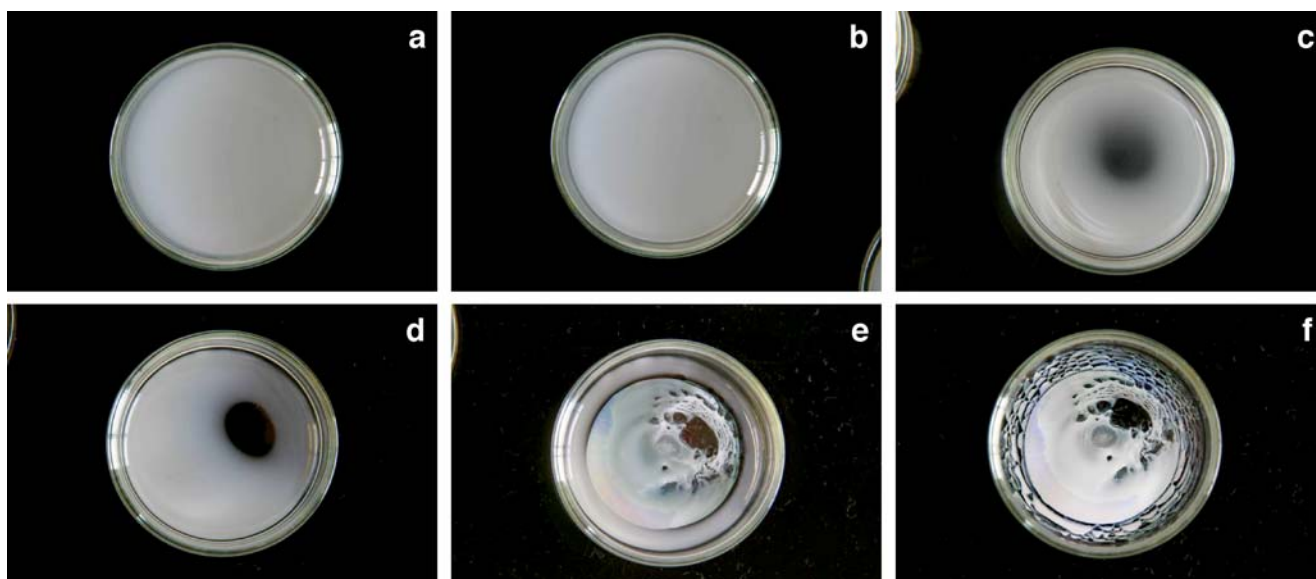
Fig. 1 Sedimentation and drying patterns of CS550 silica suspensions in a glass dish at 27 °C. $\phi = 0.000827$, 10 ml, code 211, (**a**) after 7 min, (**b**) 80 min, (**c**) 11 h, (**d**) 48 h, (**e**) 94 h, and (**f**) 165 h, dry

the suspension temperature in the upper region of the suspension. When the colloidal spheres reach the edge wall of the dish at the outside region of the liquid, a part of the spheres will turn upward and go back to the center region. However, many large and heavy spheres may drop down on the cell bottom close to the outside cell wall, in which the effective horizontal flow of the spheres may temporarily stop. This process must be followed by the broad ring accumulation of the spheres near the round outside edges.

It should be noted here that the sedimentation broad ring patterns in the liquid phase reported in this study were first observed in a glass dish in a previous study from the author's laboratory [31]. However, the broad ring formation in the dried film has been observed so often for most of the solutions and suspensions examined by our group [21–41] and also by other researchers [1, 2, 5, 9, 11, 16]. Recently, microgravity experiments were made for observing the drying dissipative patterns of a deionized suspension of the colloidal silica spheres. It is surprising to note that the broad ring patterns did not disappear even in microgravity [46]. This strongly supports the fact that both the gravitational and Marangoni convections contribute to the broad ring formation on earth, and the latter is still important in microgravity.

We should further note that the broad ring patterns, which were generally observed for all drying patterns of the suspensions and solutions on a cover glass including the present results, were already formed in the process involving the convectional flow of water and solutes in the suspension state in a glass dish. The broad ring sedimentation structures were also observed in a polystyrene dish [31], in a watch glass [32], and even a deep bowl [34] as shown in Table 1.

It should be mentioned in this study that the sharpness of the sedimentation broad rings was sensitive to the rate of change in the room temperature and/or humidity, though the pictures showing this were omitted in this report. This finding has been reported in a previous study for the first time [39]. It is highly plausible that the sedimentary spheres are surrounded by the extended electrical double layers and float and move on the cell plate, which is also surrounded by the electrical double layers, under the influence of the convectional flow of water. It is interesting to note that the sharpness of the broad rings was most sensitive for the silica spheres with 305 nm diameter [39] and then 560 nm ones in this study, while the sensitivity was low for the spheres of 1.2 μm and 160 nm diameters. It is highly plausible that the temperature- and/or humidity-sensitive changes in the sharpness of the broad ring are due to the balance of the gravitational sedimentation with the convectional flow of the spheres. The former should be stronger than the latter for the large spheres, whereas the latter is much stronger than the former for small spheres. Thus, the sedimentation patterns of the small-sized spheres should be sharp compared to that of the large spheres.

In this study, we should note that the wave-like, beautifully iridescent colored structures formed in the areas between the outside edges of the film and the inner-wall of the glass dish as shown in Fig. 1f. Similar patterns were observed for CS300 sphere suspensions for the first time [39]. The drying frontier started at the center of the glass dish and moved toward the outer cell wall with time. These wave-like patterns appeared only when the concentration of the spheres is not high enough to cover the entire cell surfaces. For the 1.2-μm diameter colloidal silica spheres, no wave-like patterns were observed. The reason for this

observation is not clear, but can be strongly correlated to the fact that the strength of the convectional flow of large spheres is much weaker compared to that of the small spheres. It should be further mentioned in this study that the iridescent colors of the dried film of CS550 spheres were not very strong compared to those of CS300 spheres. The main reason is due to the fact that the wavelength of the primary Bragg diffraction light calculated from the nearest-neighbored intersphere distance, 560 nm, is around 1000 nm and much longer than the main range of the wavelengths of the visible light.

Figure 2 shows the macroscopic drying patterns of CS550 spheres in a glass dish along with a rather large amount of sodium chloride and at 165 h after the suspensions were set. The sedimentation patterns were quite similar to those of the sphere suspensions without salt. However, the drying patterns of the former were different from the latter. The wave-like shaped patterns disappeared, but the crystal-like patterns appeared instead of the wave-like patterns for the former.

Figure 3 shows the microscopic patterns of the dried films, in which the initial sphere concentrations range from 0.00041 to 0.0083 in volume fraction and the extended pictures were taken by a metallurgical microscope. Beautiful and colorful microstructures were observed. The iridescent colors are due to the secondary Bragg diffraction of light by the crystal array of the colloidal spheres and the main cause of the microstructures will be the traces of the convectional flow of spheres and water molecules on the plate of a glass dish.

Figure 4 shows the microscopic pictures of the dried film of CS550 spheres containing sodium chloride from 0.0001 to 0.03 M. The macroscopic picture of the film was shown already in Fig. 2f. The pinkish, bluish, or greenish patterns in these pictures are composed of the silica spheres and the white patterns are the sodium chloride salt. These beautiful leaf-like patterns clearly demonstrate that the synchronous cooperative interactions between the spheres and the salt molecules on a glass dish play an important role in the pattern formation during the processes of solute solidification.

Sedimentation and drying dissipative patterns on a watch glass

When the colloidal suspension of CS550 spheres was dried on a watch glass, sedimentation of the spheres took place within 2 h especially in the upper layers of suspension and a broad ring pattern was clearly observed in the central area of the watch glass by the naked eye (see Fig. 5). The main cause for the broad ring formation is again the convectional flow of water and CS550 spheres at the different rates and due to the evaporation of water from the outer edges. The flow of spheres from the center area toward the outside edges in the lower layer of the liquid is especially important [25]. Enhancement of the convectional flow by the evaporation of water must be followed by the broad ring accumulation of the spheres near the round outside edges. We should note here that all the sedimentary spheres in the sedimentation state float above the cell plate by the repulsive interaction between the cell and spheres intermediated with the electrical double layers formed from the surfaces of the cell plate and spheres. It should be mentioned in this study that the size of the broad ring on a watch glass clearly increased during visual observations as sphere size decreased when the
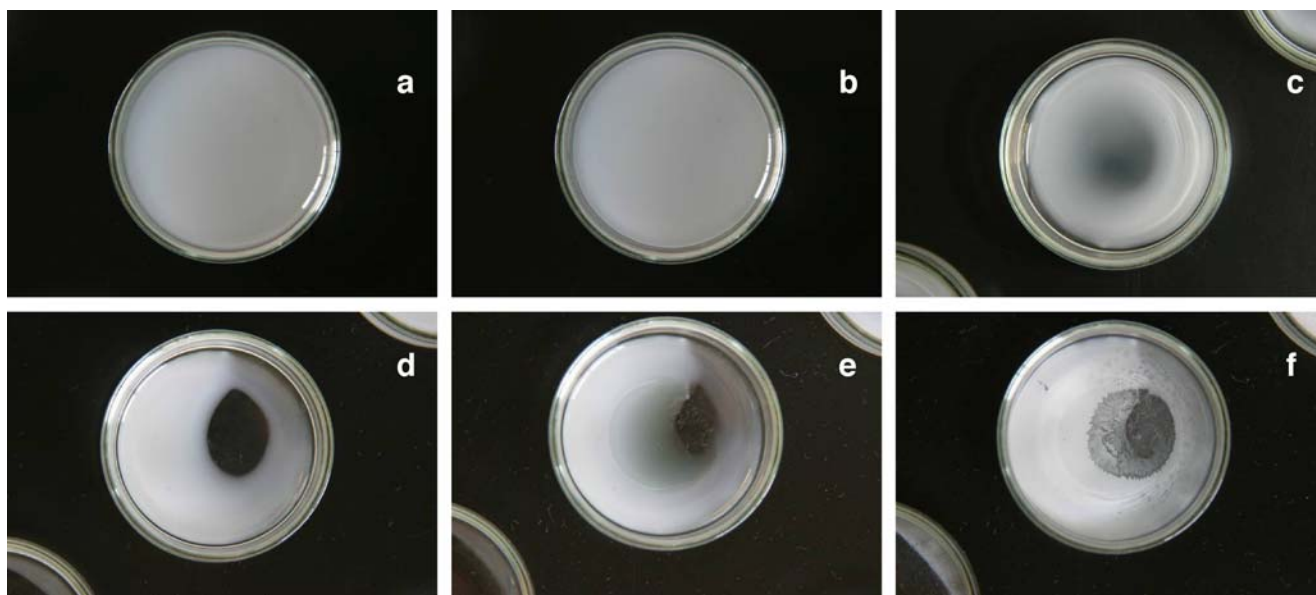

Fig. 2 Sedimentation and drying patterns of CS550 silica suspensions in a glass dish at 27 °C. ϕ =0.000827, [NaCl]=0.03 M, 10 ml, code 218, (**a**) after 7 min, (**b**) 80 min, (**c**) 11 h, (**d**) 48 h, (**e**) 94 h, and (**f**) 165 h, dry
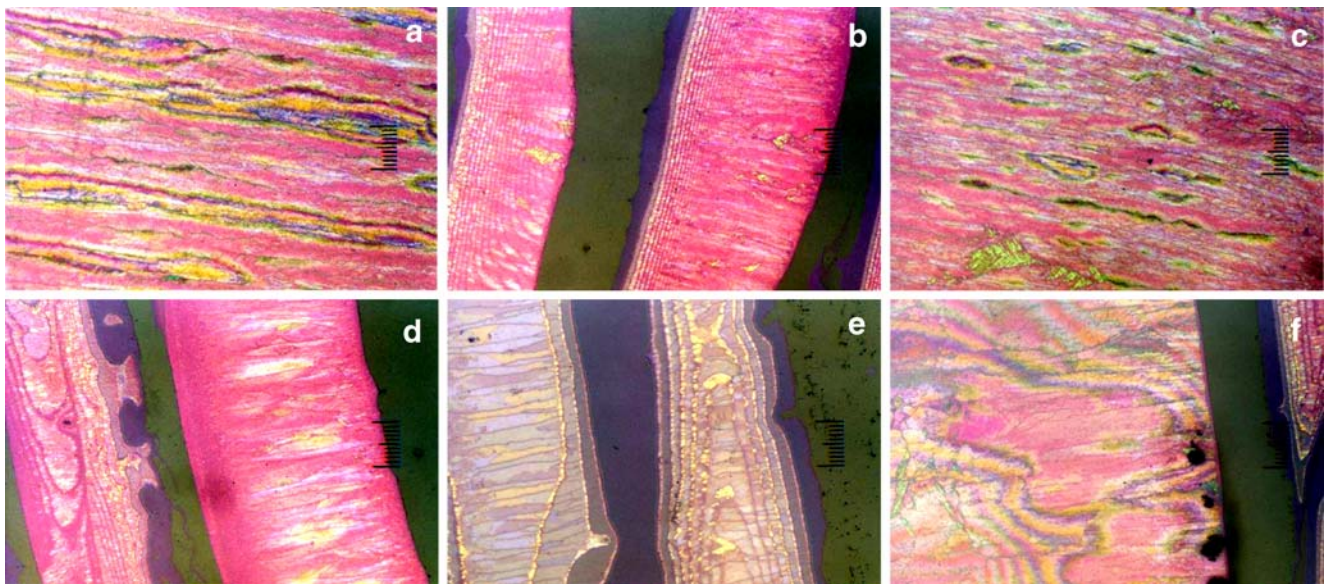
Fig. 3 Microscopic drying dissipative patterns of CS550 silica spheres in a glass dish at 27 °C. (**a**) ϕ =0.000414, (**b**) 0.00165, (**c**) 0.00248, (**d**) 0.00414, (**e**) 0.00579, and (**f**) 0.00827, 10 ml, after 122.5 h, dry

observations were compared among the examined colloidal silica spheres of 1.2 μm [32], 305 nm [39], and 560 nm diameter. This is because of the fact that the sedimentary spheres locate at positions in balance between the flow toward the outside by the convections and the inside flow by the sedimentary forces on a watch glass, and the convection flow of the smaller spheres should be much stronger. The importance of the balance was also experimentally supported from the sedimentation and drying dissipative patterns of the binary and ternary mixtures of the colloidal silica spheres having different sizes (Okubo et al., publication in preparation). A quantitative comparison of the size effects on the

convectional flow is now in progress by further adding the data of the 160-nm diameter colloidal silica spheres.

Figure 6 shows typical examples of the sedimentation and drying dissipative structures of CS550 suspension with sodium chloride on a watch glass. The sedimentation patterns were not very different between the suspensions with and without salt. However, in the presence of salt, the white sedimentation areas were smaller than those without salt. This can be explained by the decrease in the effective volume of the sedimentary CS550 spheres including the electrical double layers around the spheres by the thinning of the electrical double layers with the salt. Furthermore, the area with the
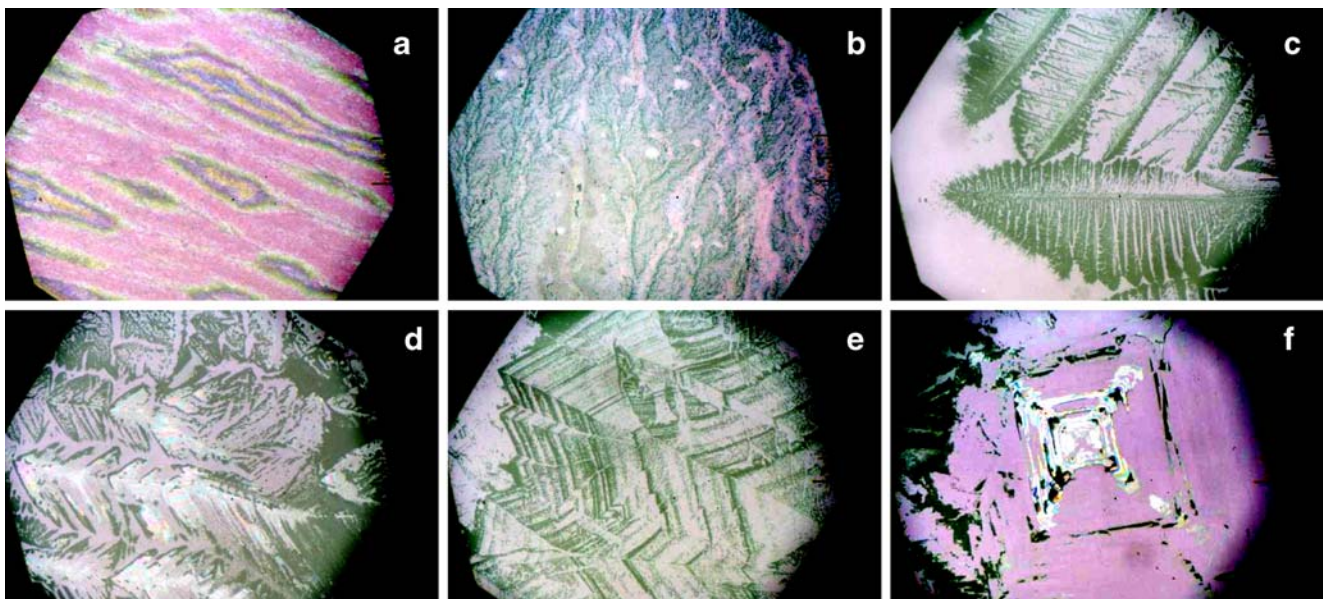

Fig. 4 Microscopic drying dissipative patterns of CS550 silica spheres in a glass dish at 27 °C. ϕ =0.000827, (**a**) [NaCl]=0.0001 M, (**b**) 0.001 M, (**c**) 0.003 M, (**d**) 0.01 M, (**e**) 0.02 M, and (**f**) 0.03 M, 10 ml, after 165 h, dry
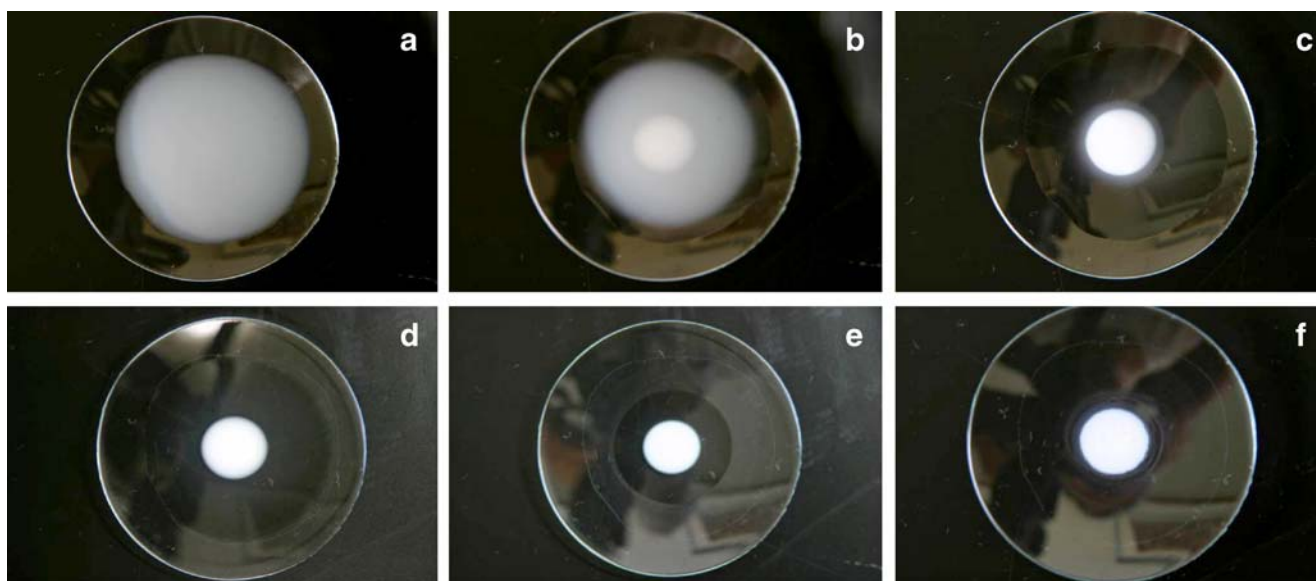
Fig. 5 Sedimentation and drying patterns of CS550 silica suspensions in a watch glass at 27 °C. ϕ =0.00207, 4 ml, code 231, (**a**) after 25 min, (**b**) 83 min, (**c**) 3.6 h, (**d**) 8.2 h, (**e**) 21 h, and (**f**) 31.5 h, dry

white drying patterns of the suspensions with salt significantly extended compared to those without salt.

Figure 7 shows the microscopic drying patterns of CS550 suspensions without salt at φ=0.00207 from the central area (subpanel a) to right-hand side outer edge (subpanel i). Two different types of microscopic patterns appeared from the central to outer edge regions, i.e., (1) round weakly iridescent colored and fine circle-like patterns in the central area, and (2) multi-string circle-like patterns in the wide outer regions. It should be noted that the type (2) patterns were observed for the suspensions containing the other silica spheres (305 nm and 1.2 μm in diameter) on

a watch glass [32, 39]. These two types of microstructures support the existence of the two different modes of convectional flows of water and solutes depending on the areas of the watch glass.

Figure 8 shows the microscopic pictures of the drying dissipative patterns in the presence of sodium chloride from the central area (subpanel a) to the outside edge (subpanel i). The central area from subpanel a to the left-hand side of subpanel c shows the weakly iridescent colors from the colloidal spheres, which may support the idea that the main component of the central area is CS550 spheres. The outer regions from the right-hand side of subpanel c to subpanel i
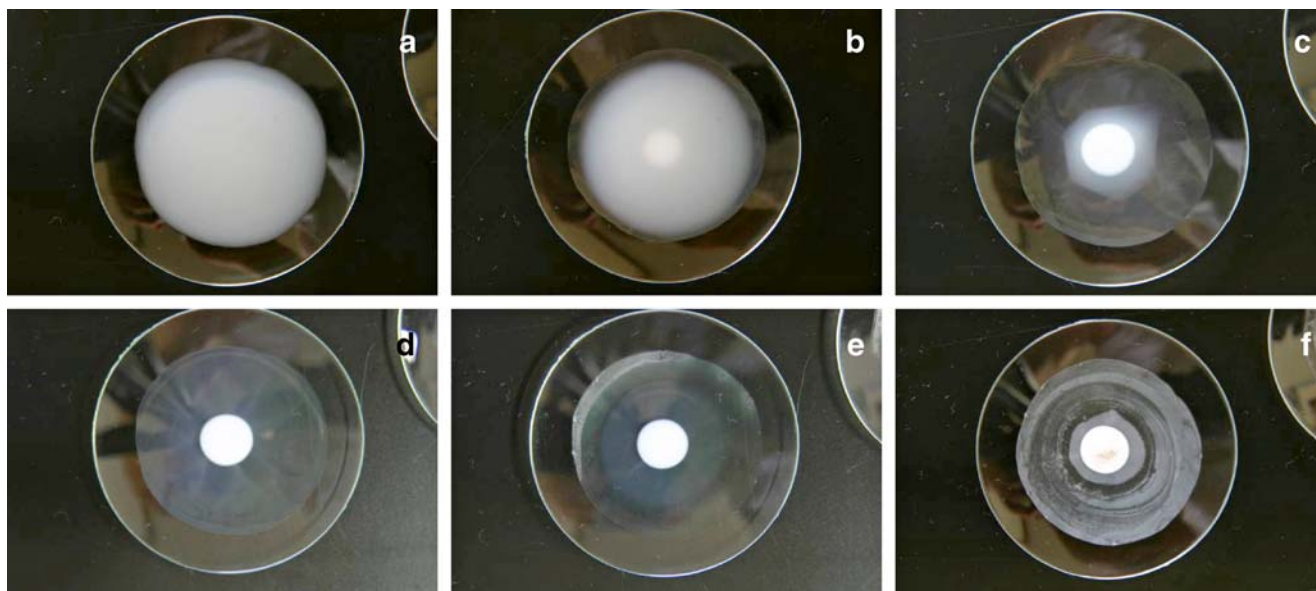

Fig. 6 Sedimentation and drying patterns of CS550 silica suspensions in a watch glass at 27 °C. ϕ =0.00207, [NaCl]=0.025 M, 4 ml, code 238, (**a**) after 25 min, (**b**) 83 min, (**c**) 3.6 h, (**d**) 8.2 h, (**e**) 21 h, and (**f**) 31.5 h, dry
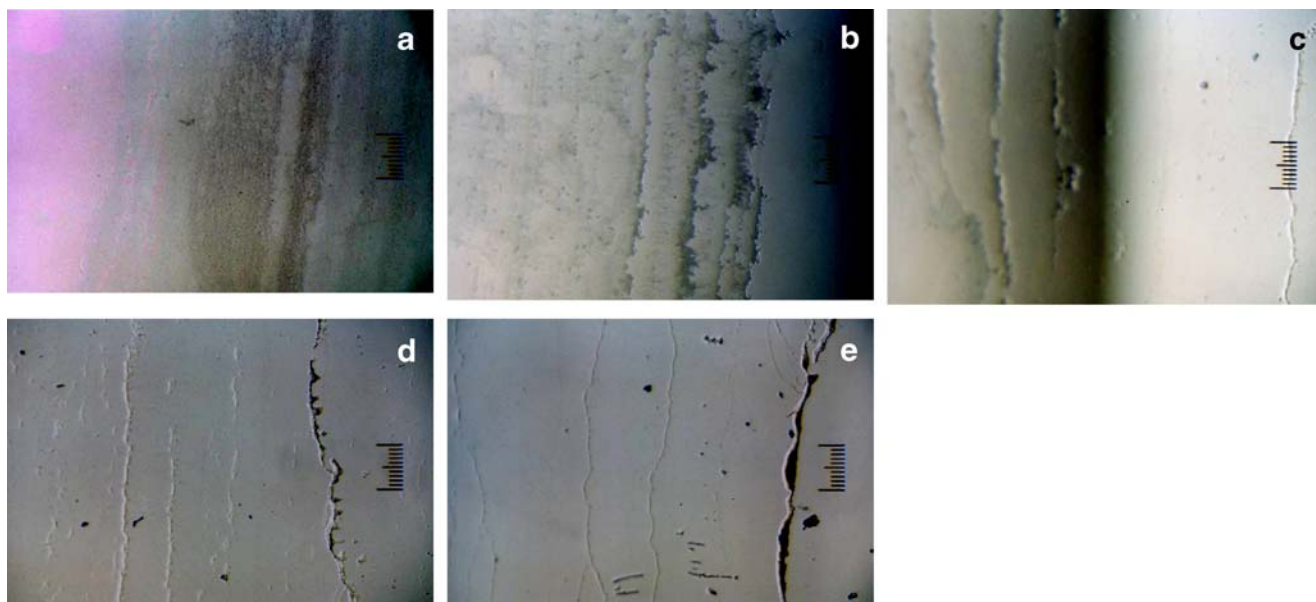
Fig. 7 Microscopic drying dissipative patterns of CS550 silica spheres in a watch glass at 27 °C. (**a**) ϕ =0.00207, 4 ml, dry, code 231, from the center (**a**) to outside edge (**e**), full scale: 0.2 mm
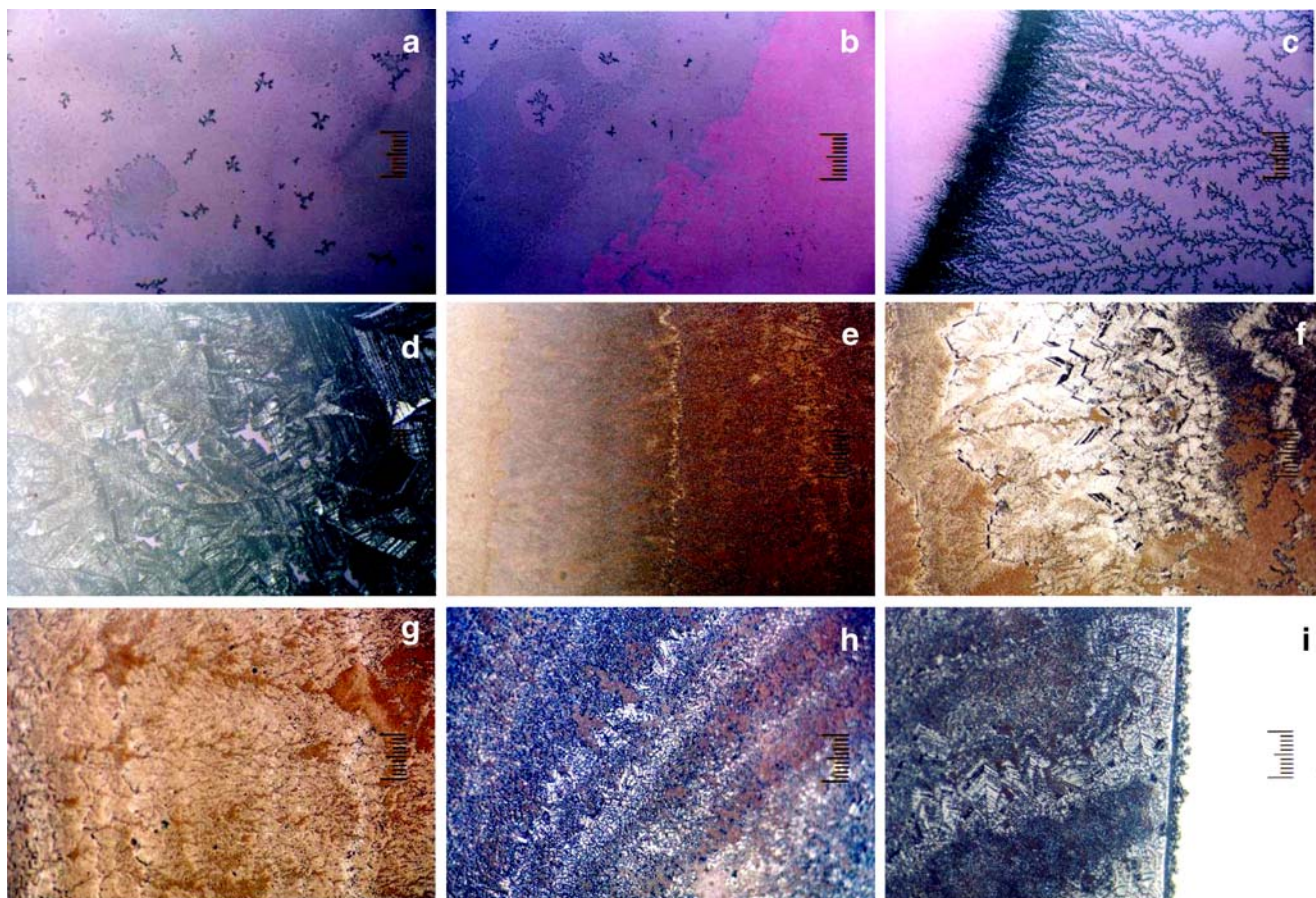

Fig. 8 Microscopic drying dissipative patterns of CS550 silica spheres in a watch glass at 27 °C. (**a**) ϕ =0.00207, [NaCl]=0.025 M, 4 ml, dry, code 238, from the center (**a**) to outside edge (**i**), full scale: 0.2 mm

showed various shapes of the complex formation between colloidal spheres and sodium chloride. Furthermore, changes in the patterns as a function of the distance from the center clearly support that the amount of salt increased as the distance from the center increased. The importance of the size segregation effect in the drying processes for sodium chloride toward the outer regions is again supported in the mixtures of the colloidal silica spheres and sodium chloride especially on a watch glass.

References

1. Vanderhoff JW, Bladford, EB, Carrington WK (1973) J Polym Sci Polym Symp 41:155
2. Nicolis G, Prigogine I (1977) Self-organization in non-equilibrium systems. Wiley, New York
3. Cross MC, Hohenberg PC (1993) Rev Mod Phys 65:851
4. Adachi E, Dimitrov AS, Nagayama K (1995) Langmuir 11:1057
5. Ohara PC, Heath JR, Gelbart WM (1998) Langmuir 14:3418
6. Uno K, Hayashi K, Hayashi T, Ito K, Kitano H (1998) Colloid Polym Sci 276:810
7. Gelbart WM, Sear RP, Heath JR, Chang S (1999) Faraday Discuss Chem Soc 112:299
8. van Duffel B, Schoonheydt RA, Grim CPM, De Schryver FC (1999) Langmuir 15:957
9. Maenosono S, Dushkin CD, Saita S, Yamaguchi Y (1999) Langmuir 15:957
10. Brock SL, Sanabria M, Suib SL, Urban V, Thiyagarajan P, Potter DI (1999) J Phys Chem 103:7416
11. Nikoobakht B, Wang ZL, El-Sayed MA (2000) J Phys Chem 104:8635
12. Ge G, Brus L (2000) J Phys Chem 104:9573
13. Chen KM, Jiang X, Kimerling LC, Hammond PT (2000) Langmuir 16:7825
14. Lin XM, Jaenger HM, Sorensen CM, Klabunde KJ (2001) J Phys Chem 105:3353
15. Kokkoli E, Zukoski CF (2001) Langmuir 17:369
16. Ung T, Liz-Marzan LM, Mulvaney P (2001) J Phys Chem 105:3441
17. Haw MD, Gilli M, Poon WCK (2002) Langmuir 18:1626
18. Narita T, Beauvais C, Hebrand P, Lequeux F (2004) Eur Phys J E Soft Matter 14:287
19. Tirumkudulu MS, Russel WB (2005) Langmuir 21:4938
20. Shimomura M, Sawadaishi T (2001) Curr Opin Colloid Interface Sci 6:11
21. Okubo T, Okuda S, Kimura H (2002) Colloid Polym Sci 280:454
22. Okubo T, Kimura K, Kimura H (2002) Colloid Polym Sci 280:1001
23. Okubo T, Kanayama S, Ogawa H, Hibino M, Kimura K (2004) Colloid Polym Sci 282:230
24. Okubo T, Kanayama S, Kimura K (2004) Colloid Polym Sci 282:486
25. Okubo T, Kimura H, Kimura T, Hayakawa F, Shibata T, Kimura K (2005) Colloid Polym Sci 283:1
26. Okubo T, Yamada T, Kimura K, Tsuchida A (2005) Colloid Polym Sci 283:1007
27. Yamaguchi T, Kimura K, Tsuchida A, Okubo T, Matsumoto M (2005) Colloid Polym Sci 283:1123
28. Kimura K, Kanayama S, Tsuchida A, Okubo T (2005) Colloid Polym Sci 283:898
29. Okubo T, Shinoda C, Kimura K, Tsuchida A (2005) Langmuir 21:9889
30. Okubo T, Yamada T, Kimura K, Tsuchida A (2006) Colloid Polym Sci 284:396
31. Okubo T (2006) Colloid Polym Sci 284:1395
32. Okubo T (2006) Colloid Polym Sci 284:1191
33. Okubo T (2006) Colloid Polym Sci 285:231
34. Okubo T (2006) Colloid Polym Sci 285:331
35. Okubo T, Itoh E, Tsuchida A, Kokufuta E (2006) Colloid Polym Sci 285:339
36. Okubo T, Nozawa M, Tsuchida A (2007) Colloid Polym Sci 285:827
37. Okubo T, Kimura K, Tsuchida A (2007) Colloids Surf 56:201
38. Okubo T, Onoshima D, Tsuchida A (2007) Colloid Polymer Sci 285:999
39. Okubo T, Okamoto J, Tsuchida A (2007) Colloid Polym Sci 285:967
40. Okubo T, Nakagawa N, Tsuchida A (2007) Colloid Polym Sci (in press) DOI 10.1007/s00396-007-1678-9
41. Okubo T, Yokota N, Tsuchida A (2007) Colloid Polymer Sci (in press) DOI 10.1007/s00396-007-1681-1
42. Terada T, Yamamoto R, Watanabe T (1934) Proc Imp Acad (Tokyo) 10:10
43. Terada T, Yamamoto R, Watanabe T (1934) Sci Pap Inst Phys Chem Res Jpn 27:75
44. Terada T, Yamamoto R (1935) Proc Imp Acad (Tokyo) 11:214
45. Ball P (1999) The self-made tapestry formation in nature. Oxford Univ Press, Oxford
46. Tsuchida A, Okubo T (2003) Sen'I Gakkaishi 59:264